PHYSICAL REVIEW B VOLUME 25, NUMBER 9 1 MAY 1982

Spin-resolved scattering in the Cu(Mn) magnetic-impurity system

R. H. Hendel,* R. J. Higgins, and C. G. Lin-Hendel*
Department of Physics, University of Oregon, Eugene, Oregon 97403
(Received 2 April 1981)

We report spin-resolved scattering measurements on the Cu(Mn) magnetic-impurity system using the third-harmonic de Haas—van Alphen wave-shape—analysis technique (dHvA WA). Magnetic field and temperature dependences of spin-up and spin-down scattering and the magnetic-moment—conduction-electron interaction H_{ex} are presented. The exchange field H_{ex} is found not to scale with H/T. The H and T dependences of the spin-resolved scattering agree qualitatively with existing theories and spin-averaged experimental data such as the negative magnetoresistivity. The spin-resolved d-impurity scattering phase shifts derived from our data agree with results obtained by other, complementary methods. Fundamental dHvA amplitude measurements are presented on all symmetry orbits. For the low-field data, a partial-wave shift analysis indicates predominately d-type impurity scattering. The high-field data deviate from a linear extrapolation of the low-field data on all orbits. The magnetic field where the deviation occurs scales with the amount of d wave present in that orbit.

INTRODUCTION

Classic approaches to understanding magnetic impurities in metals have ignored realistic band structures in order to remain tractable and to explain dominant features of the problem (i.e., the Kondo effect). Measurements have largely been of bulk properties such as resistance and susceptibility, where microscopic information is averaged out. For example, investigations of scattering and the impurity-moment—conduction-electron exchange have been made via negative magnetoresistivity measurements.[1] The scattering and exchange energy are important parameters which characterize both the real and imaginary parts of the impurity's interaction with the host. Bulk magnetoresistance averages the scattering over both spins and over the entire Fermi surface. This allows determination of only a single estimate of the exchange integral J.[2]

Theories explaining the suppression of the Kondo divergence in a magnetic field are rather successful in a system such as Cu(Cr).[3] The potential scattering V is ignored, appropriate for the Cu(Cr) system, which has no spin dependent scattering.[4] Cu(Cr), however, is not the rule but the exception. Most other magnetic impurity systems show spin dependent impurity scattering. Recent calculations[5] have shown the importance of V and explain the strong suppression of the Kondo divergence by a magnetic field in Cu(Mn). Recent experiments also give a finer picture which matches advances in the theory. Notions such as the Friedel oscillations around a magnetic impurity, a spin-dependent impurity d resonance, and localized versus itinerant magnetic moment have now been experimentally demonstrated.

The measurement of satellite Knight shifts in nuclear magnetic resonance (NMR) by Cohen and Slichter[6,7] directly demonstrates Friedel oscillations around the impurity. Using an impurity scattering phase-shift calculation, Cohen and Slichter construct a spin-dependent density of states for the Mn magnetic impurity. A significant result is the nearly integer number of d electrons localized at the impurity. Cohen and Slichter's phase-shift calculation, however, neglects the host band structure—the Cu host was assumed to be a free-electron gas. An independent corroboration of the numerical results is thus desirable.

Very recently, Zeller *et al.*[8] have presented self-consistent Korringa-Kohn-Rostoker (KKR)—Green's-function (i.e., model-independent) calculations of the electronic and magnetic structure of $3d$ impurities. Zeller's results for Cu(Mn) resemble, in position and width, the gross features of the spin-dependent resonance $N(S,E)$ calculated by Cohen and Slichter.[6,7] Zeller's density of states,

though, exhibits additional structure consistent with hybridization of the impurity energy bands with the Cu host d bands. The two calculations disagree on the values of $N(S,E_F)$ at the Fermi level. In the Cohen calculation, the $\downarrow$ band is nearly full, with $N(\downarrow,E_F)\simeq 0$, while Zeller's result states

$$N(\downarrow,E_F)/N(\uparrow,E_F)\simeq 0.3 \ .$$

Since these parameters dominate the transport properties, their independent determination is of interest.

The de Haas–van Alphen (dHvA) effect probes scattering parameters and the exchange energy local in $\vec{k}$ space. This complements the NMR satellite data which are local in $\vec{r}$ space. Earlier dHvA measurements of the g shift[4] allow a determination of the exchange energy. Scattering rates on different orbits (s,p,d like) allow the projection of the orbital moment dependence of the impurity-host interaction. With dHvA wave-shape analysis, scattering rates can also be spin resolved,[9,10] which provides a direct comparison with the theoretically calculated spin-resolved density of states.

Early dHvA measurements of spin-averaged impurity scattering in Cu(Mn) (Ref. 11) gave anomalously low values, a factor of more than 2 smaller than inferred from the impurity resistivity. These measurements used the slope of the dHvA amplitude $\ln(A)$ vs $1/H$ plot to extract the scattering temperature. However, the total dHvA amplitude is the sum of spin-up and spin-down contributions. It is convenient to view the dHvA oscillation as the projection of a rotating vector.[9,10] When a magnetic impurity is present, the magnitudes of the individual spin contributions as well as the angle between the spin-up and spin-down vectors can vary independently with H. The resultant magnitude of the fundamental dHvA amplitude alone is not sufficient to describe the system, and the conventional $\ln(A)$ vs $1/H$ determination of the scattering rate is likely to be in error.

By measuring the harmonic content of the dHvA signal, the relative amplitudes as well as their relative phases, it is possible to uniquely determine the spin-up scattering, the spin-down scattering, and the exchange field at a single magnetic field and temperature. The first three harmonics are sufficient to deduce these quantities, even in the presence of a moderate amount of additional harmonic content from magnetic interaction.[12] This technique, which has come to be known as wave-shape analysis (WA), is described in detail in the literature.[13–15] Measurements of the harmonic content of the dHvA oscillations can be made as a function of T and H, facilitating comparison with bulk measurements over the Kondo transition. Although dHvA WA results are restricted to relatively high fields (>30 kG) and low temperatures (<2 K) where sufficient harmonic content is available, the spin-resolved scattering is new information not available from other methods at this time. Resistivity measurements require the subtraction of the phonon contribution from the scattering. Phonon scattering is absent in the dHvA lifetime measurement.[16,17] A potentially large source of error is thus eliminated.

The advantages mentioned above make the dHvA WA technique an attractive tool to obtain the H,T dependences of the spin-resolved electron scattering and the conduction-electron–magnetic-moment exchange interaction in the Cu(Mn) system. Our WA measurements are restricted to the neck orbit in Cu to avoid the complication of an excessive magnetic interaction contribution to the harmonic content of the dHvA signal. Although not as representative of "bulk" conduction electrons as the belly orbit, the orbit symmetry character is well known for Cu, and scaling laws for other orbits have already been demonstrated for the exchange energy[4] and for the scattering rates.[18] Such scaling is also present in our dHvA fundamental amplitude measurements made on all symmetry orbits. We observe a field dependence which scales with orbital symmetry character and explains the earlier anomalously low scattering rates measured by Coleridge[11] in Cu(Mn).

EXPERIMENTAL METHODS

Magnetic impurity information in the dHvA effect—WA

dHvA oscillations, periodic variations of the magnetization with $1/H$, can be described in the presence of magnetic impurities as

$$\tilde{M}=\sum_{\sigma}\sum_{r=1}^{\infty} C_r D^r E^{\sigma r}\sin[2\pi r(F/H-\gamma) + p\pi/4-\sigma\pi r S'] \ , \quad (1)$$

where r is the dHvA harmonic index, σ is $+1$ (-1) for spin up (down) electrons, and C_r is the dHvA amplitude reduction factor due to finite

temperature; for the neck orbit $p=+1$. The amplitude reduction due to spin-averaged and spin-dependent scattering is accounted for by D and E:

$$D=\exp(-r\lambda\mu\bar{X}/H)\ , \tag{2}$$

$$E=\exp(-\lambda\mu\delta X/H)\ , \tag{3}$$

where $\bar{X}$ is the temperature equivalent of the average scattering rate and $2\delta X$ is the difference of the two scattering components, F is the dHvA frequency ($\hbar A_{\rm ext}/2\pi e$), H is the externally applied magnetic field, μ is the conduction-electron effective mass in units of the free-electron mass, and γ and λ are constants. The effect of the exchange between impurity and conduction electrons is contained in S':

$$S'=\frac{\mu}{2}(g_0-H_{\rm ex}/H)\ , \tag{4}$$

where g_0 is the orbitally averaged cyclotron g factor for the pure host metal; $H_{\rm ex}=E_{\rm ex}/\mu_B$ describes the change of the energy level spacing between up spin and down spin due to the magnetic impurity.

Equation (1) can be rewritten in terms of relative phase shifts $\Delta\theta_r$ induced by the magnetic impurity[9]:

$$\tilde{M}=\sum_{r=1}^{\infty}A_r'C_rD^r\sin[2\pi r(F/H-\gamma)+p\pi/4+\Delta\theta_r+(1-q_r')\pi/2]\ , \tag{5}$$

where

$$A_r'=\tfrac{1}{2}[E^{2r}+E^{-2r}+2\cos(2\pi rS')]^{1/2}\ , \tag{6}$$

$$\Delta\theta_r=\tan^{-1}[\tan(\pi rS')\tanh(r\lambda\mu\delta X_D/H)]\ , \tag{7}$$

$$q_r'=\pm1 \quad \text{for} \quad \cos(\pi rS')\gtrless 1\ . \tag{8}$$

The conduction electrons are affected by the sum of the externally applied field and the induced oscillatory crystal magnetization:

$$B=H+4\pi(1-n)\tilde{M}\ , \tag{9}$$

where n is the effective demagnetization factor. This effect is known as the magnetic interaction (MI) effect. Substituting B for H in Eqs. (5)–(7) results in an implicit equation for $\tilde{M}$ which can be solved[13–15] in the "weak MI" limit

$$|k'A_1'C_1D_1|<<1\ . \tag{10}$$

The result links two relative phases $2\theta_1-\theta_2$, $3\theta_1-\theta_3$ and the amplitude ratio A_3A_1/A_2^2 with the physical parameters of interest: the exchange parameter S', the spin scattering anisotropy δX, and the spin-averaged scattering temperature $\bar{X}$ at a given H and T.

Computer-generated theoretical plots of the three observables as a function of S' at different values of δX intersect with the experimentally measured values of the observables. This results in a unique and consistent range of possible solutions for S' and δX as shown in Figs. 1(a)–1(c). These calculated curves are not symmetric around $S'=0$ because of the magnetic interaction effect discussed above. The curves also give a good indication on the sensitivity of S' and δX to changes of the observables. The exact solution is then obtained by a second computer program which further steps and varies S' and δX at finer resolution and calculates the three observables for each set of S' and δX until the calculated values agree with the measured values to within experimental error. The average scattering temperature $\bar{X}$ is then derived from the ratio of the second dHvA harmonic amplitude to the dHvA fundamental.

Possible errors due to the skin effect[21] can be corrected for in the dHvA WA method by measuring the deviation of the observed dHvA amplitude dependence on the modulation current with the expected Bessel-function dependence.[10] A detailed discussion can be found in Ref. 22.

Considerations for dHvA fundamental amplitude measurements

Measurements of orbital scattering anisotropy have been extremely useful in the past. It has been shown that this anisotropy generally scales with the d character of the host wave function.[4,18] Unfortunately, the WA method cannot be extended to orbits other than the neck in Cu. Strong magnetic interaction and a decreased harmonic content due to higher effective masses make WA measurements impractical on orbits other than the neck in Cu. The fundamental dHvA amplitude measurement is thus the only access to the information on orbital scattering anisotropy even though complications due to the magnetic field dependence of $\bar{X}$ and its spin components will complicate the interpretation.

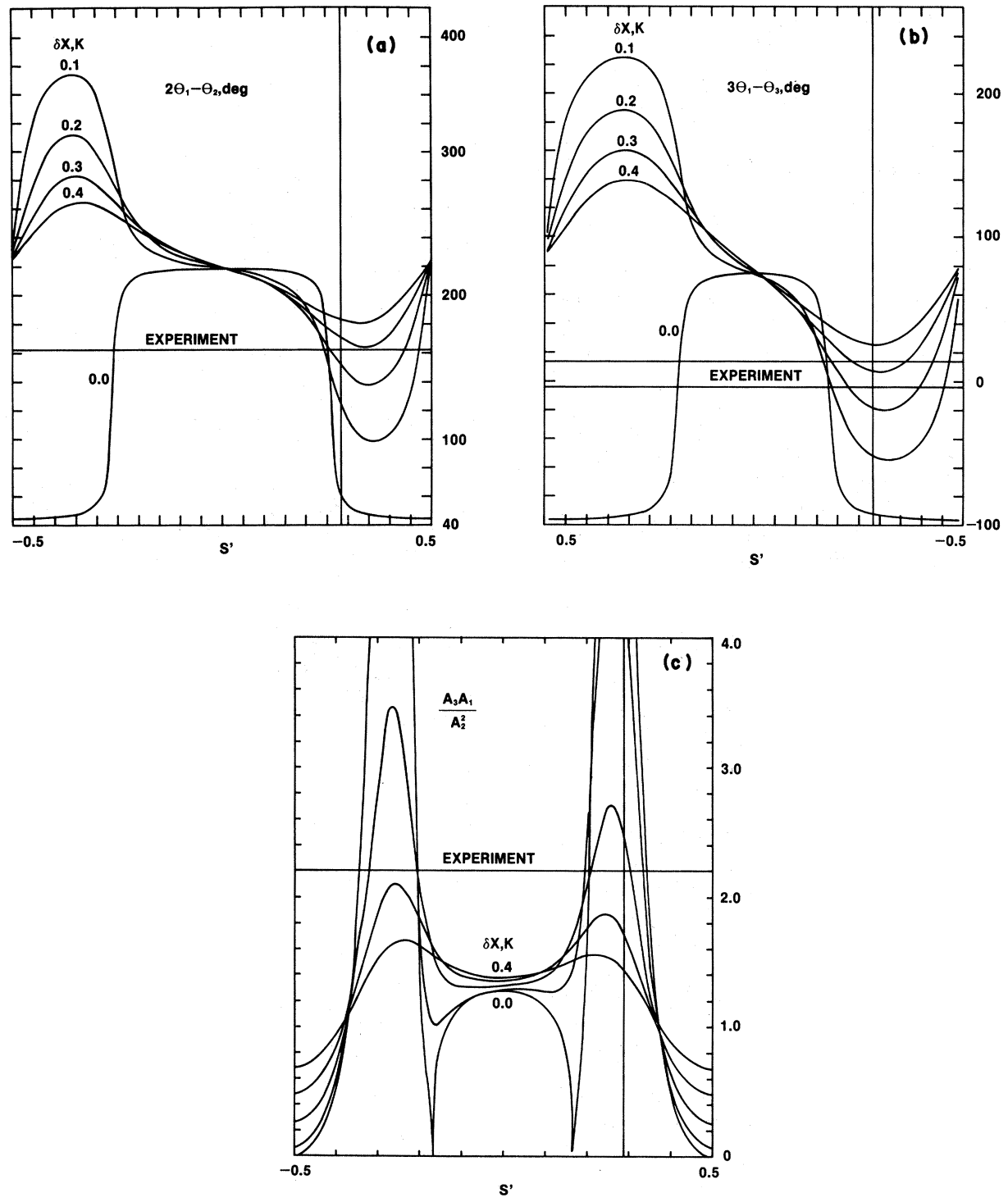

FIG. 1. Plot of dHvA WA experimental observables: (a) $2\theta_1-\theta_2$, (b) $3\theta_1-\theta_3$, (c) A_1A_3/A_2^2 vs the exchange parameter S' for various δX. The curves are theoretically calculated from an expansion of the oscillatory magnetization. The experimentally measured dHvA amplitudes A_1,A_2,A_3 and phases $2\theta_1-\theta_2$, $3\theta_1-\theta_3$ yield a self-consistent set of S' and δX as indicated in these plots. The horizontal lines across the plots are the experimentally measured values of respective observables. The vertical lines indicate the common solution S' for the three plots which yield $S'=0.28$ and $\delta X=0.25$. Once S' and δX are determined, $\bar{X}$ can be derived from the ratio of the second and first dHvA harmonic amplitudes A_2/A_1.

MEASUREMENTS AND DISCUSSION OF RESULTS

Sample preparation

Sample crystals were grown from 99.999% Cu plates and high-purity Mn flakes. A master alloy was grown of approximately 2300 at. ppm Mn and diluted to yield the desired impurity concentration during subsequent Bridgeman growth.

The impurity content in the sample must be high enough such that background scattering due to crystal imperfections and undesired trace impurities is negligible. Impurity-impurity interactions set an upper limit to the concentration range possible.

Low-field magnetization measurements[19] show impurity-impurity interactions in Cu(Mn) crystals with 180 at. ppm Mn concentration only at temperatures below 1 K and at 100 at. ppm only at temperatures below 0.3 K. The lowest temperature investigated here was approximately 1 K. Impurity-impurity interactions are further suppressed in a high magnetic field. Transverse magnetoresistance measurements[20] show that concentrations above 70 at. ppm and below 3300 at. ppm are well behaved, showing the expected concentration independent linear dependence of $\Delta\rho_H/(\rho)_{H=0}$ vs H^2. The concentration selected for our measurements, 120 at. ppm, is therefore free from impurity interaction effects.

After growth the crystals are oriented using Laue x-ray backscattering and cut to sample size by spark erosion. Parts of the crystal adjacent to the samples are used for concentration determination by chemical analysis.

Three samples of the 120 at. ppm Mn concentration have been used for the measurements. The results from all samples fall within the experimental errors quoted below. We have also used a reference sample with approximately 60 at. ppm Mn to confirm the scaling of the dHvA fundamental amplitude scattering temperatures (X_D) with concentration and found X_D to be proportional to the concentration within experimental error. For clarity in the figures, we limit the discussion here to results from a single sample.

Results and empirical comparisons

The spin-resolved scattering data obtained by third harmonic wave-shape analysis are shown in Figs. 2–5. The two spin components differ by as

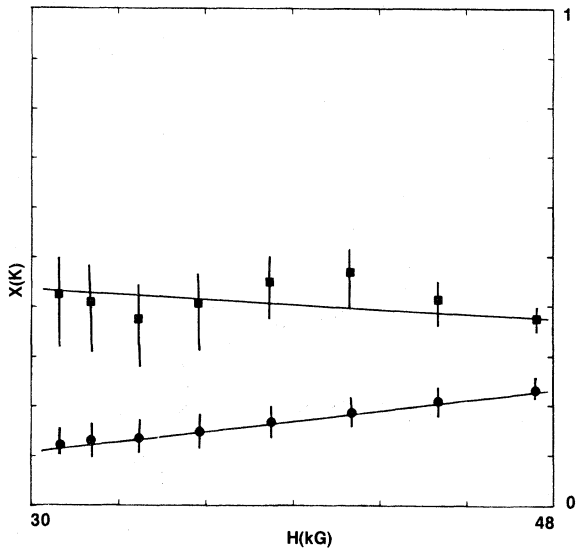

FIG. 2. Magnetic field dependence of the spin-averaged scattering temperatures $\bar{X}=(X\uparrow+X\downarrow)/2$ (■) and the scattering anisotropy $\delta X=(X\uparrow-X\downarrow)/2$ (●) at constant temperature ($T=1.18$ K). The error bars at low fields account for a $\pm5°$ error in the relative phases $2\theta_1-\theta_2$, $3\theta_1-\theta_3$ and a 5% error in each harmonic amplitude A_1,A_2,A_3. At high fields the dHvA signal-to-noise ratio is significantly higher. The measured relative phases and amplitudes are thus more accurate than those at low fields. The phase error is reduced to $\pm2°$ and the amplitude error to 2%.

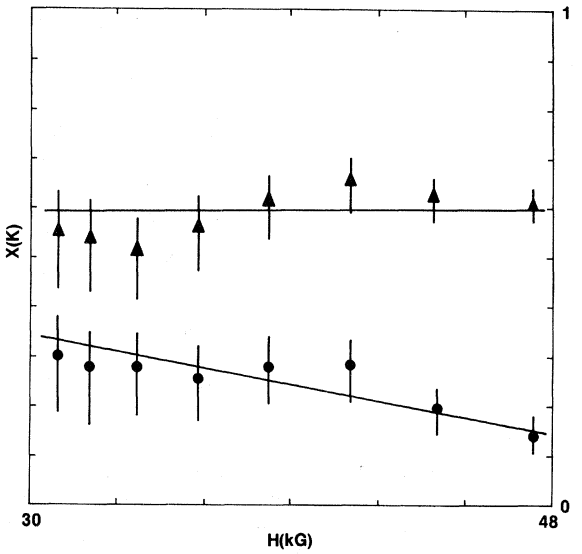

FIG. 3. Magnetic field dependence of the spin-up (▲) and the spin-down (●) scattering components at constant temperature ($T=1.18$ K).

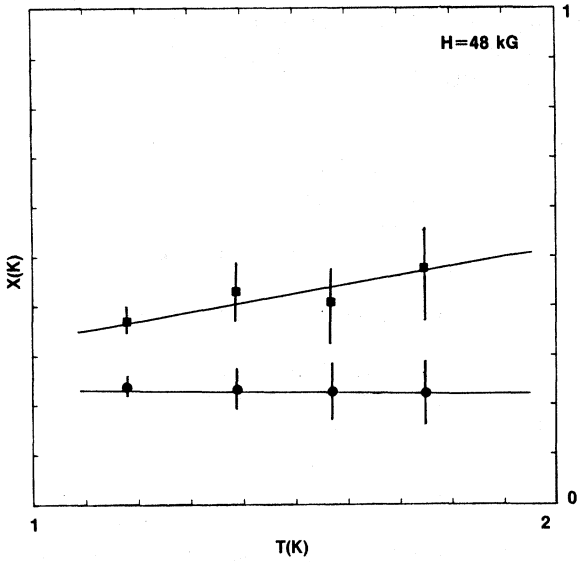

FIG. 4. Temperature dependence of the spin-averaged scattering temperature $\bar{X}$ (■) and the spin-scattering anisotropy δX (●) at constant magnetic field ($H=48$ kG).

much as a factor of 3, a significantly larger spin dependence than, for example, the 30% observed in Cu(Fe).[10] This is consistent with the previous inferences[4,11] that the transport properties are dominated by scattering from a single spin component of the Mn d resonance. We have found that the spin-up electrons are scattered stronger. This can be explained by the larger density of states for the up-spin.[6–8] The ratio of spin-up to spin-down scattering rates at high magnetic fields should be proportional to the spin-up to spin-down ratio of the density of states, since the spin-split scattering is frozen out and the electronic scattering is dominantly elastic. Our results numerically agree with the 0.3 ratio obtained in Zeller's[8] calculations and disagree with Cohen's[6,7] result of a nearly zero down-spin density of states.

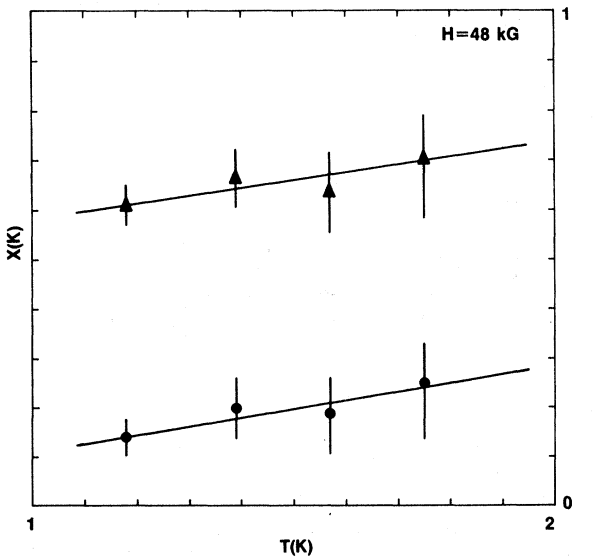

FIG. 5. Temperature dependence of the spin-up (▲) and spin-down (●) scattering components at constant magnetic field ($H=48$ kG).

The spin-up scattering displays negligible field-dependence, giving a zero slope to the straight-line fit shown (Fig. 3). The spin-down scattering component, however, shows a strong magnetic field dependence, decreasing with increasing magnetic field. Both spin components of scattering increase with increasing temperature, at rates $dX_{\uparrow}/dT=0.15$ and $dX_{\downarrow}/dT=0.17$ (Fig. 5). The slight nonlinearity in the H dependences of the scattering parameters may be evidence of a field dependence possibly more complex than indicated by the least-squares straight-line fit shown.[32] Any deviations from linearity are comparable to or less than the error bars.

Let us compare these results with existing scattering data,[1] obtained from measurements of the temperature and magnetic field dependence of the negative magnetoresistivity (Ref. 1, Fig. 1). The dominant contribution to the conductivity, hence to the negative magnetoresistivity, is the spin component with the smaller scattering rate. We observe (Fig. 3) a decrease of the spin-down scattering with increasing magnetic field. This is consistent with the negative magnetoresistance results.[1] We find (Fig. 5) an increase of the spin-down scattering (at constant H) with increasing temperature, opposite to the usual "Kondo slope" where $dR/dT<0$ (R is the resistivity). This, however, is consistent with the magnetoresistance measurements where a positive slope, $(dR/dT)_H>0$, is found at these values of H and T. The suppression of the Kondo effect at higher magnetic fields is stronger than the $\ln(T)$ term. The relative rates of change of the scattering versus temperature and magnetic field are shown in Table I for Monod's magnetoresistance data[1] and our results. The fact that our measurements show very strong H and T dependences of the scattering rate can be inferred by an extrapolation of the magnetoresistance results of Monod at lower fields to the higher fields of our measurements.

The magnetic field and temperature dependences of the exchange field H_{ex} are shown in Figs. 6 and 7. Here,

TABLE I. Comparison of the temperature and magnetic field dependences of scattering for Monod's negative magnetoresistance measurements and our dHvA wave-shape analysis measurements. The scattering rate and resistivity are described in units of $1/\tau$, where τ is the electronic lifetime.

	$\frac{d(\tau^{-1})}{dT} / \frac{1}{\tau}$	$\frac{d(\tau^{-1})}{dH} / \frac{1}{\tau}$
Monod, Ref. 1	0.01 K^{-1} at 10 kG ($\langle T \rangle = 1.5$ K) 0.03 K^{-1} at 20 kG	-0.0286 kG^{-1} at $\langle H \rangle = 5$ kG ($T = 1.8$ K) -0.0294 kG^{-1} at $\langle H \rangle = 15$ kG
This work	0.78 K^{-1} at 50 kG ($T = 1.5$ K)	-0.032 kG^{-1} at 1.2 K ($H = 48$ kG)

$$H_{ex} = -\frac{cJC_L}{\mu_B} \langle S_z \rangle , \tag{11}$$

where c is the impurity concentration in units of atomic fraction, C_L is the orbital d-wave scattering contribution, J is the exchange integral describing the s-d interaction, and $\langle S_z \rangle$ is the average spin component of the impurity magnetic moment along the magnetic field direction and follows a Brillouin function in H/T. Within the magnetic field range observed, H_{ex} increases much faster with increasing field than the Brillouin function which is near saturation at this H/T range. This strong field dependence is a puzzle. However, a field dependence of H_{ex} stronger than that of a Brillouin function is supported by data from other impurity systems such as Cu(Cr) (Ref. 4) and Au(rare-earth metal) (Refs. 13 and 29). Our result adds to the growing amount of experimental evidence that the field dependence of H_{ex} does not follow a Brillouin function in H/T.

Even though H_{ex} has not reached its saturation value, we use the maximum value of H_{ex} from our measurements to derive a lower limit for the exchange integral J from Eq. (11). Assuming $\langle S_z \rangle$ to be saturated and using[30] $C_L = 0.383$ gives $J > 2$ eV. To compare our value derived from a static spin polarization experiment to a value obtained from scattering data, it must be divided by a factor of $2L + 1$.[4] This correction yields $J_{eff} > 0.4$ eV, in

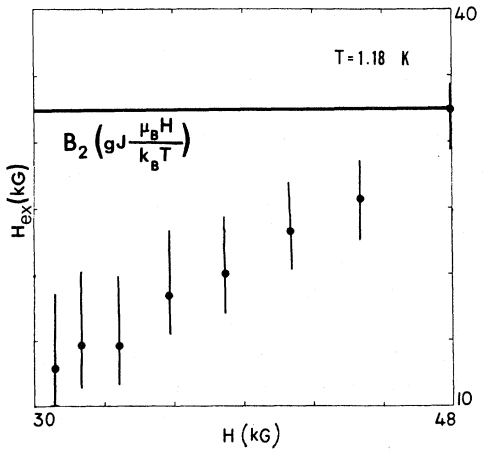

FIG. 6. Exchange field H_{ex} vs the applied magnetic field at constant temperature ($T = 1.18$ K). The field dependence is much stronger than the corresponding Brillouin function for $\langle S_z \rangle$ which is also shown in the figure. The Brillouin function is scaled to fit the H_{ex} value at the highest magnetic field measurement where H_{ex} is closest to saturation.

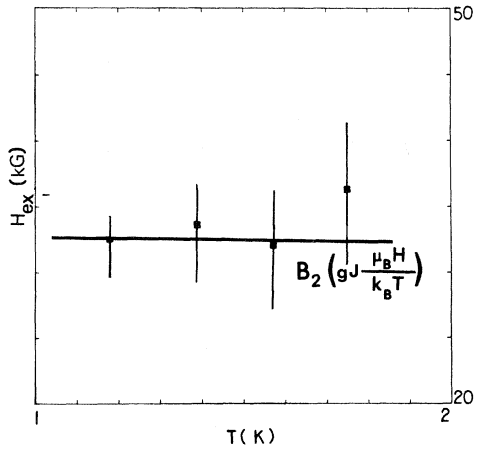

FIG. 7. Temperature dependence of the exchange field H_{ex} at constant magnetic field ($H = 49$ kG). Within the error bars, no temperature dependence is observed. The solid line indicates the temperature dependence of the corresponding Brillouin function for $\langle S_z \rangle$.

agreement with Monod's result of $J=0.4\pm0.1$ eV.[1]

In contrast, H_{ex} is approximately constant over the experimental range of T with H held constant (Fig. 7). These results indicate that the exchange field does not scale with H/T in the Cu(Mn) impurity system over the range of T and H investigated. Relatively few other dHvA data are available for comparison. H/T scaling of the exchange field was observed in spin-split zero (SSZ) measurements of Cu(Cr).[4] The SSZ, however, is an accidental cancellation of dHvA amplitude which occurs only when the spin-up component is of the same magnitude but out of phase with the spin-down component. The strong spin dependence of the impurity scattering in Cu(Mn) results in a spin-split minimum (SSM) which is completely washed out with only a few ppm Mn. No measurements of H and T dependences of H_{ex} were reported in earlier SSM measurements on Cu(Mn).[4] We therefore resolve to theoretical interpretations of our observations.

Comparison with exchange scattering theory

Theoretical attempts to explore the magnetic field and temperature dependence of spin-resolved scattering and the exchange interaction are proposed by Mulimani[23] and Harris *et al.*[24] The model uses a modified *s-d* exchange Hamiltonian, limits the exchange to a *d-d* interaction, and includes potential scattering. Explicit field and temperature dependences of physical parameters, however, are only obtained in the limit where the potential scattering and other complications of the exchange interaction are neglected. Following Shiba's notation,[25] Mulimani and Harris describe H_{ex}, δX, and $\bar{X}$ in terms of a complex self-energy:

$$\Sigma_\sigma=\Sigma'_\sigma+i\,\mathrm{sgn}\Sigma''_\sigma\ , \tag{12}$$

where $\sigma=\uparrow,\downarrow$ represent the conduction-electron spin. The dHvA physical parameters are then expressed in terms of either real or imaginary part of that self-energy:

$$\bar{X}\propto-\tfrac{1}{2}(\Sigma''_\uparrow+\Sigma''_\downarrow)=[C\pi\rho(-J/2)^2S(S+1)]-\left[C\langle S_z\rangle(-J/2)^2\pi\rho\tanh\left[\frac{Q}{2k_BT(\pi+1)}\right]\right]$$

$$-(C2\pi\rho^2(-J/2)^3S(S+1)\ln\{[Q^2+(\pi+1)^2(k_BT)^2]/D^2\})\ , \tag{13}$$

$$\left.\begin{matrix}H_{ex}\\ \delta X\end{matrix}\right\}\propto\tfrac{1}{2}(\Sigma''_\uparrow-\Sigma''_\downarrow)=c(-J/2)\langle S_z\rangle\left[1-(-J/2)\rho\ln\left[\frac{Q^2+(\pi+1)^2(k_BT)^2}{D^2}\right]\right]\ , \tag{14}$$

where

$$\langle S_z\rangle=\sum_{S_z}S_ze^{S_zQ/k_BT}\Big/\sum_{S_z}e^{S_zQ/k_BT}\ , \tag{15}$$

$$Q=g\mu_BH\ . \tag{16}$$

D is determined from the Kondo temperature and characterizes the width of a rectangular density of states (ρ).

The neglect of potential scattering is a serious deficiency since it implies that there is no spin dependent scattering,[24] $\delta X=0$. This is obviously not the case here. For a qualitative interpretation of the measurements we shall assume initially that the temperature and magnetic field dependence is at least qualitatively similar to Eqs. (13) and (14) even when potential scattering is nonzero.

The spin-averaged scattering temperature $\bar{X}$ in Eq. (13) is composed of three terms:

(i) $C\pi\rho(-J/2)^2S(S+1)$,

which is independent of magnetic field and temperature.

(ii) $-C\langle S_z\rangle(-J/2)^2\pi\rho\tanh[Q/2k_BT(\pi+1)]$,

which describes the freeze-out of spin flip scattering, which in a strong magnetic field is energetically unfavorable.

(iii) $C2\pi\rho^2(-J/2)^3S(S+1)\ln\{[Q^2+(\pi+1)^2(k_BT)^2]/D^2\}$,

which is the Kondo term.

δX and H_{ex} in Eq. (14) are composed of two terms:

(iv) $C(-J/2)\langle S_z\rangle$

and

(v) $-C(J/2)^2\langle S_z\rangle\rho\ln\{[Q^2+(\pi+1)^2(k_BT)^2]/D^2\}$.

The freeze-out term of $\bar{X}$ (ii) has a tanh factor which increases the temperature dependence over that of (iv). The temperature-dependent contribution of the Kondo term opposes that of (ii) and (iv). When the Kondo term is not negligible, its influence is more apparent on (iv) than on (ii) since (iv) is less temperature dependent than (ii). The temperature dependence of H_{ex} and δX should therefore be less than that of $\bar{X}$. This is consistent with our observation (Figs. 4 and 7). Within experimental error, no temperature dependence is observed for both the exchange field H_{ex} and δX. In contrast, $\bar{X}$ increases with rising temperature. The fact that the two observables show different behavior suggests that the $\tanh[Q/2k_BT(\pi+1)]$ term is important. Since the tanh saturates for H/T values of similar magnitude that cause saturation of $\langle S_z\rangle$, this observation implies that $\langle S_z\rangle$ is not saturated. The field-dependence measurement confirms this. Strong field dependence of the exchange field and δX is seen in Figs. 2 and 6 in agreement with the lack of saturation in the magnetoresistance.[26] The slight decrease in $\bar{X}$ as the magnetic field increases is expected by the freezeout of spin-flip scattering. This is even more clearly evident in the spin-resolved results where $X_\downarrow$ displays a strong decrease with H while $X_\uparrow$ is nearly constant. This is also consistent with the recent calculations of the Mn resonance,[6–8] where the density of impurity states at E_F is large for the spin-up states but small for the spin-down states. Elastic (hence field-independent) scattering should dominate for the up-spin conduction electrons, while the down-spin electrons will have a contribution from spin-flip scattering (hence a decreasing function of H).

Since H_{ex} and δX have equivalent functional dependences on H and T, Mulimani's theory predicts that the ratio $\mu_BH_{ex}/\delta X$ is a constant. Figure 8 shows the magnetic field dependences of H_{ex}, δX, and their ratios. In spite of considerable changes in H_{ex} and δX, their ratio is approximately constant. Within the experimental error bars, however, a drift to higher values is observed. Chung *et al.*[27] have observed a similar behavior in the Au(Fe) system. The prediction of the constancy of $\mu_BH_{ex}/\delta X$ seems approximately but not precisely true.

The freeze-out term for spin-flip scattering scales as a function of H/T whereas the Kondo term does not. The observed violation of the H/T scaling in the exchange data discussed above might also be due to the influence of potential scattering.

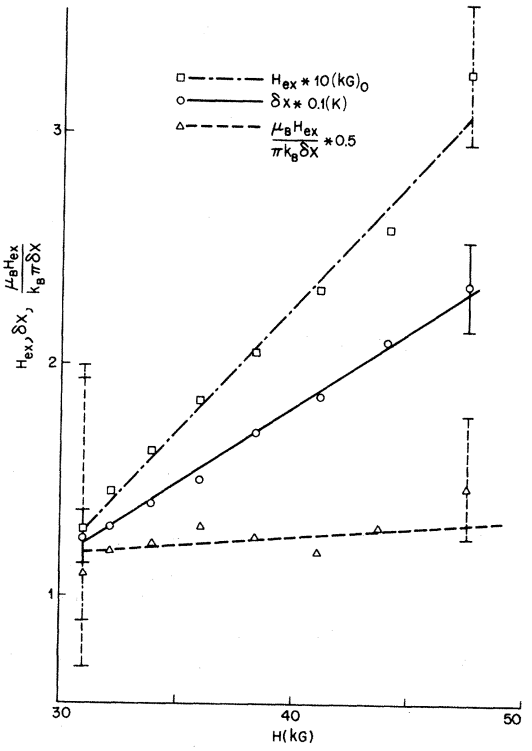

FIG. 8. Magnetic field dependence of δx (○), H_{ex} (□), and their ratio $\mu_BH_{ex}/k_B\pi\delta x$ (△). In order to fit all three curves on the same graph, δx is scaled times 0.1, H_{ex} times 10, and $\mu_BH_{ex}/k_B\pi\delta x$ times 0.5. While δx and H_{ex} show strong magnetic field dependence, $\mu_BH_{ex}/k_B\pi\delta x$ is nearly constant.

A finite potential scattering is a necessary condition for finite spin-dependent scattering.[23,25] Since the values of δX (Fig. 2) are a sizable fraction of the total scattering, potential scattering must also be sizable. Keiter and Kurkijärvi[5] have calculated the influence of potential scattering on the magnetoresistivity and have shown that it can strongly influence magnetic field and temperature dependences. In Fig. 9 we plot the results of Ref. 8 separately for three different phase shifts in order to clarify the effect of potential scattering. The enhancement of the Kondo term is surprising for $T >> T_K$, where bare moment behavior is expected. However, it has been shown[1] that in the presence of potential scattering and exchange the effects of the Kondo term can persist to temperatures well above T_K. In the absence of potential scattering we can see from Fig. 9 that the applied magnetic field simply suppresses the unitary limit plateau, as observed in Cu(Cr).[28] With moderate potential scattering (phase shift 20°), an applied field reverses the sign of the slope dR/dT from the normal Kondo effect and results in the H and T dependences of Monod's measurements[1] on Cu(Mn).

Impurity phase-shift determination

A Friedel-Anderson model used by Shiba[25] provides a transparent connection between dHvA physical parameters $\bar{X}$, δX, and H_{ex} and impurity scattering phase shifts. The Friedel-Anderson model does not provide magnetic field and temperature dependences, but will allow us to extract *spin-dependent* impurity phase shifts for comparison with recent calculations.[6–8]

Shiba describes the scattering and exchange in terms of a complex self-energy which can be related to dHvA parameters.[29] By expressing the self-energy in terms of impurity phase shifts in the Friedel-Anderson model, a direct connection is found between dHvA parameters and impurity phase shifts:

$$\frac{\mu}{2}g' = \frac{\mu_B H}{\hbar\omega_c}\left[g_0 + \frac{a_{\rm orb}(5c/\pi\rho_0)}{\mu_B H}(\sin\delta_\uparrow\cos\delta_\uparrow - \sin\delta_\downarrow\cos\delta_\downarrow)\right], \tag{17}$$

$$\bar{X} = a_{\rm orb}\frac{5c}{2\pi^2 k_B\rho_0}(\sin^2\delta_\uparrow + \sin^2\delta_\downarrow), \tag{18}$$

$$\delta X = a_{\rm orb}\frac{5c}{2\pi^2 k_B\rho_0}(\sin^2\delta_\uparrow - \sin^2\delta_\downarrow), \tag{19}$$

$$\frac{\Delta F}{F} = -\frac{a_{\rm orb}5c}{2\pi\rho_0\hbar\omega_c}(\sin\delta_\uparrow\cos\delta_\uparrow + \sin\delta_\downarrow\cos\delta_\downarrow). \tag{20}$$

Since there is no temperature or field dependence contained in Eqs. (17)–(19), the determination of the scattering phase shifts $\delta_\uparrow$ and $\delta_\downarrow$ suggests the use of observables or combination of observables that are nearly field and temperature independent. $\bar{X}$ and $H_{ex}/\delta X$ fulfill that requirement. Using Eq. (18) directly and forming the ratio of Eqs. (17) and (19) yields

$$\bar{X}\frac{2\pi^2 k_B\rho_0}{5ca_{\rm orb}} = \sin^2\delta_\uparrow + \sin^2\delta_\downarrow, \tag{21}$$

$$\frac{h\omega_c S' - g_0\mu_B H}{2\pi k_B\delta X} = \frac{\sin\delta_\uparrow\cos\delta_\uparrow - \sin\delta_\downarrow\cos\delta_\downarrow}{\sin^2\delta_\uparrow - \sin^2\delta_\downarrow}. \tag{22}$$

We estimate $a_{\rm orb}$, the anisotropy of the *s-d* mixing, as 0.54 (appropriate for this orbit[30]) and use the free-electron value of 0.17 eV^{-1} for ρ_0. Taking an average scattering temperature of 0.4 K and the high-field, low-temperature values of S' and δX ($S'=0.282$, $\delta X=0.233$ at $H=47.6$ kG and $T=1.18$ K) gives

$$\delta_\uparrow = 0.18\pi, \quad \delta_\downarrow = 0.88\pi.$$

Using the Friedel sum rule

$$Z_d = 5/\pi(\delta_\uparrow + \delta_\downarrow), \tag{23}$$

$$2S = 5/\pi(\delta_\downarrow - \delta_\uparrow), \tag{24}$$

results in

$$Z_d = 5.2, \quad S = 1.7.$$

These values are compared to those of other measurements in Table II. Considering the simpli-

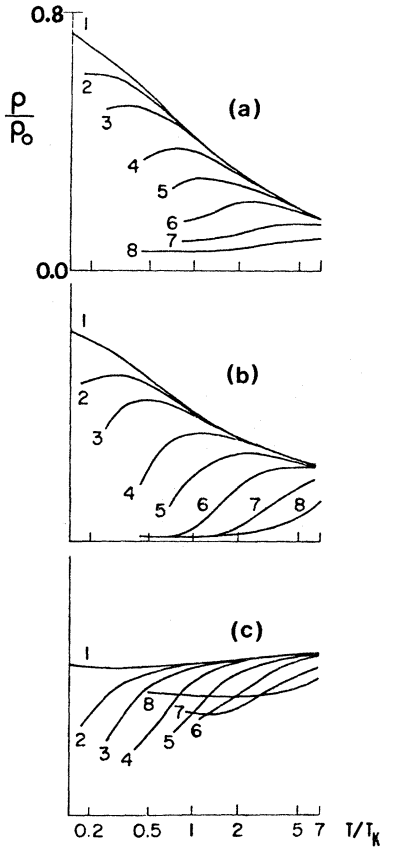

FIG. 9. Magnetoresistivity for various magnetic fields as a function of temperature (extracted from Ref. 5, Fig. 5). Both magnetic field and temperature are normalized to their Kondo values. The curves are separated for three values of potential scattering: (a) 0°, (b) 20°, (c) 45°. The eight curves for each value of potential scattering correspond to the following B/B_K values: 1, 0; 2, 0.09; 3, 0.18; 4, 0.44; 5, 0.88; 6, 1.76; 7, 3.52; 8, 7.05.

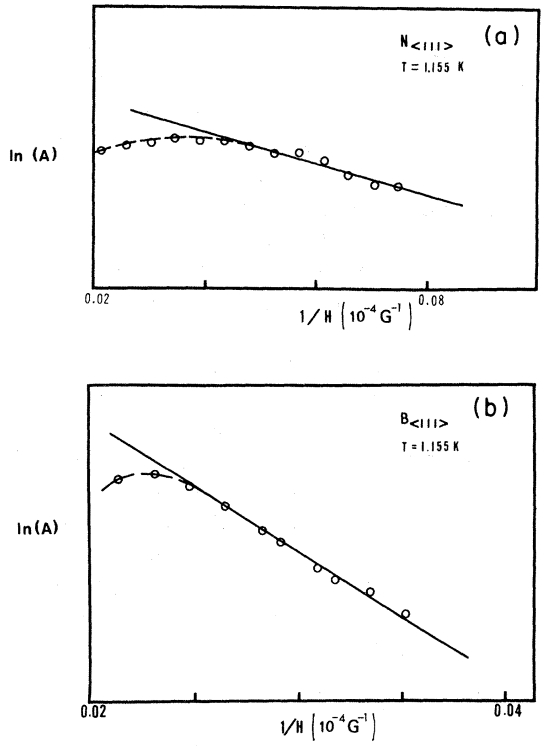

FIG. 10. Dingle plots [ln(dHvA amplitude) vs $1/H$] for the (a) neck $N_{\langle 111\rangle}$ and (b) belly $B_{\langle 111\rangle}$ orbits in Cu(Mn) 120 at. ppm at $T=1.155$ K. Both plots show a curvature starting at a characteristic magnetic field H_d which scales with the amount of d character present at each orbit (see also Table V).

city of the model (only the $L=2$ phase shift is used), the overall agreement is quite good. The down-spin phase shift, though, is smaller than the values obtained by NMR.[6] This indicates a less than totally filled majority-carrier spin band which agrees better with the calculations of Zeller *et al.*[8] Since the dHvA measurement only probes within $\pm k_B T$ of E_F, it is not possible to derive a density of states versus energy plot as was done by Cohen and Slichter and by Zeller *et al.* However, the dHvA approach in obtaining phase shifts is much more direct than that of Cohen and Slichter. Their approach leads to the spin-resolved density of states not directly from the data but from a complex, iterative fit. Our results indicate that the majority-spin band lies higher than that calculated

TABLE II. Comparison of spin-resolved impurity scattering phase shifts obtained from different methods. The Friedel sum Z_d, impurity spin S, and impurity resistivity ρ derived from the phase shift are also noted.

Method	Z_d	S	$d\uparrow/\pi$	$d\downarrow/\pi$	Impurity resistivity ($\mu\Omega$ cm/at. %)
Resistivity	5.73	1.95	0.18	0.96	2.76
NMR	5.5	2	0.15	0.95	2.1
dHvA WA	5.2	1.7	0.18	0.88	3.8

TABLE III. Values for $\cos(\pi S')$ at the orbits used for the partial-wave phase-shift analysis. A spurious curvature in the $\ln(A)$ vs $1/H$ plot could occur if the measurement was made close to a spin-split zero or spin-split minimum. We have used the measured exchange field at the neck and scaled it with the d-like part of the orbit character to the other orbits. The results indicate all orbits sufficiently far from a spin-split zero or minimum that the change of angle between the individual spin components can be neglected to a first approximation.

	$N_{\langle 111\rangle}$	$B_{\langle 111\rangle}$	$B_{\langle 100\rangle}$	$R_{\langle 100\rangle}$	$D_{\langle 110\rangle}$
$\cos(\pi S')$	0.645	−0.34	−0.659	−0.612	−0.426

by Cohen but lower than that predicted by Zeller. This observation also offers an explanation to the lack of spectral evidence for the Mn d resonance in Cu.[31]

Orbital dependence of scattering (dHvA fundamental amplitude measurements)

There are two limits where conventional (slope) scattering temperatures are physically meaningful in magnetic impurity systems: Either one spin dominates completely (total SDS) or both spin components are equal (no SDS) and the phase between the two individual spin components does not change. The wave-shape results presented earlier (Fig. 2) suggest that the value of δX might be sufficiently small at low magnetic fields to warrant the "no SDS" condition. A calculation of the angle between the individual spin components shows that each orbit is far from the condition of a spin-split minimum (see Table III) and therefore indicates that the change of the angle between the individual spin components can be neglected in a first approximation. Figures 10(a) and 10(b) give two examples of characteristic features observed in amplitude plots of all symmetry orbits. In the low magnetic field range, the curves appear straight and allow the determination of a conventional scattering temperature X_D, listed in Table IV. At the high field a characteristic curvature is found in all samples on all symmetry orbits measured. The departure from the linear extrapolation of the low-field data occurs at a characteristic field H_d (defined as the field where the amplitude is reduced to $1/e$ of the extrapolated value). The magnitude of H_d scales with the amount of d wave in the corresponding orbit. This result is shown in Table V. To compare with the orbital character, all H_d values are normalized to the $B_{\langle 111\rangle}$ orbit which shows the most d character. The observed curavature also explains the anomalously low scattering values reported earlier[11] which are less than half of the values expected from resistivity measurements.

TABLE IV. Low-field Dingle scattering temperatures for Cu(Mn) 120 at. ppm. The upper field limit indicates the highest field value used in the linear $\ln(A)$ vs $1/H$ fit. The errors are large because the number of points available for each fit was less than that in a typical Dingle slope scattering determination which shows no high-field deviation from a straight line.

Orbit	X_D (K)	Upper field limit (kG)
$N_{\langle 111\rangle}$	0.38±0.2	15.6
$B_{\langle 111\rangle}$	1.06±0.1	37
$B_{\langle 100\rangle}$	0.89±0.15	34
$R_{\langle 100\rangle}$	0.90±0.15	34
$D_{\langle 110\rangle}$	1.12±0.1	37

TABLE V. d-wave scaling of the "deviation field" described in the text. The values quoted for the orbital character stem from derivatives each dHvA extremal orbit with respect to the s, p, and d scattering phase shifts:

$$\frac{\partial A}{\partial \eta_l} \Big/ \sum_l \left[\frac{\partial A}{\partial \eta_l}\right]_{\text{orb}} .$$

These values are obtained from fits to the well-known band structure of Cu and are estimated to be $<1\%$ (Ref. 30).

Orbit	Orbit character s	p	d	d character scaled to $B_{\langle 111\rangle}$	H_d (kG)	$\frac{H_d}{H_{dB_{\langle 111\rangle}}}$
$B_{\langle 111\rangle}$	6.8	22.4	70.8	1	45.45	1
$B_{\langle 100\rangle}$	8.6	27.0	64.4	0.91	43.48	0.96
$D_{\langle 110\rangle}$	5.9	35.6	70.7	0.998	45.45	1
$R_{\langle 100\rangle}$	5.3	30.4	64.3	0.908	38.46	0.85
$N_{\langle 111\rangle}$	0	61.7	38.3	0.541	24.39	0.54

Phase-shift analysis calculation

The partial-wave phase-shift analysis of dHvA scattering data has been valuable in obtaining orbital anisotropy of the partial wave (s,p,d) scattering, at least in nonmagnetic impurity systems. The results of a partial-wave phase-shift analysis of the orbital scattering anisotropy data using an approach by Coleridge[30] are shown in Table VI. The scattering is predominately d-like. The "d-wave only" phase shift fits the data within experimental error. The experimental error of about 10% is significantly greater than typical dHvA scattering measurements because the linear $\ln(A)$ vs $1/H$ region contains only few data points thus increasing the uncertainty. Adding a p-wave contribution im-

TABLE VI. Partial-wave phase shifts for d-wave only scattering, p- and d-wave scattering and s,p,d-wave scattering. The C_L values are parameters returned from the fitting program (Ref. 30); δ_s, δ_p, δ_d are the impurity phase shifts in units of π. rms and χ^2 are measures of the quantity of the fit. The impurity resistivity obtained from the fit is also shown. The value for d-wave scattering alone agrees with our value obtained from the dHvA WA (Table II). The d-wave contribution clearly dominates in all three cases.

	d wave only	p,d wave	s,p,d wave
c_0	0	0	0.08
c_1	0	0.03	0.02
c_2	0.18	0.18	0.17
δ_s/π	0	0	−0.068
δ_p/π	0	−0.062	−0.041
δ_d/π	−0.146	−0.144	−0.142
rms (%)	15.9	25.7	20.6
χ^2 (%)	9.6	8.2	8.3
$\rho\left[\frac{\mu\Omega\,cm}{\text{at. \%}}\right]$	4.0	3.0	2.9

proves the value of the resistivity yet worsens the rms quality of the fit. Allowing the s-wave phase shift to vary improves the rms deviation slightly and further improves the value of the resistivity. The fit is insensitive to the s-wave contribution since the partial derivatives $dA_0/d\eta_L$ give the d-wave contribution a factor of 10 more weight than the s-wave contribution. So, even when the s-wave phase shift amounts to 50% of the d-wave phase shift, its contribution to the scattering is only 5%.

This lends support to the assumption of d-wave scattering used to derive spin-resolved scattering phase shifts in the preceding section. The reason that the fit is not improved when a p-wave contribution is allowed is presumably due to the fact that the curvature of the $\ln(A)$ vs $1/H$ data is largest for the neck orbit, which is the most p-like. It is reasonable to assume that the low-field region, which is below the accessible field range of our apparatus, would have a steeper slope and thus higher scattering temperature. Our experimental result likely underestimates the scattering for this orbit and thus the contribution of the p character to the scattering.

Thus, in summary, even though magnetic interaction prevents the determination of exchange and spin-resolved scattering on orbits other than the neck, the scaling with orbital d character observed in the deviation field H_d and the low-field amplitude scattering data suggests a certain degree of universality for the wave-shape analysis results on the neck orbit.

CONCLUSIONS

We have presented magnetic field and temperature dependences of the conduction-electron—magnetic-moment exchange and the spin-resolved scattering obtained by third harmonic dHvA wave-shape analysis. The results are consistent with previous spin- and orbitally-averaged negative magnetoresistance measurements. The exchange field does not scale with H/T. The presence of strong spin-dependent scattering is evidence for the importance of potential scattering in the Cu(Mn) system.

With the assumption of pure d-wave scattering we have obtained spin-up and spin-down impurity phase shifts *without* using resistivity, Friedel sum, or impurity spin as input. Conventional $\ln(A)$ vs $1/H$ plots show prominent features which scale with the amount of d-wave character present in the respective orbit. The curvature observed explains the anomalously low scattering temperatures reported previously on the neck orbit. In the low-field limit the slope scattering temperatures of the orbits measured can be related to partial-wave shifts between the host and the impurity. The analysis shows that the scattering is indeed dominantly d-like.

ACKNOWLEDGMENTS

We thank Dr. Y. Chung and Professor D. Lowndes for the use of their partial-wave determination program. Professor Lowndes's continuous interest is also gratefully recognized. Dr. L. S. Cheng, Dr. Tom Matheson, and Dr. Peter Deimel assisted with portions of the data-acquisition system. The research was supported by NSF Division of Materials Research and the Tektronix Foundation.

---

*Currently at Tektronix Laboratories, Tektronix Inc., Beaverton, Oregon 97077.

[1]P. Monod, Phys. Rev. Lett. 19, 1113 (1967).
[2]N. Karnezos and J. A. Gardner, Phys. Rev. B 9, 3106 (1974); F. W. Smith, *ibid.* 14, 241 (1976).
[3]M. T. Beal Monod and R. A. Weiner, Phys. Rev. 154, 540 (1967).
[4]P. T. Coleridge, G. B. Scott, and I. M. Templeton, Can. J. Phys. 50, 1999 (1972).
[5]H. Keiter and J. Kurkijärvi, Z. Phys. B 26, 169 (1977).
[6]J. D. Cohen and C. P. Slichter, Phys. Rev. Lett. 40, 129 (1978).
[7]J. D. Cohen and C. P. Slichter, Phys. Rev. B 22, 45 (1980).
[8]R. Zeller, R. Podloucky, and P. H. Dederichs, Z. Phys. 38, 165 (1980).
[9]H. G. Alles, R. J. Higgins, and D. H. Lowndes, Phys. Rev. Lett. 30, 705 (1973).
[10]H. G. Alles and R. J. Higgins, Phys. Rev. B 9, 158 (1974).
[11]P. T. Coleridge and I. M. Templeton, Can. J. Phys. 49, 2449 (1971).
[12]A. B. Pippard, Proc. R. Soc. London 272, 192 (1963).
[13]C. Lin-Hendel, Ph.D. thesis, University of Oregon, 1978 (unpublished). Available on microfilm from University Microfilms, Ann Arbor, Mich.
[14]R. J. Higgins and D. H. Lowndes, in *Electrons at the Fermi Surface,* edited by M. Springford (Cambridge

University Press, Cambridge, 1980), p. 393.
[15]Y. Chung, D. H. Lowndes, and C. Lin-Hendel, J. Low Temp. Phys. 32, 599 (1978).
[16]S. Engelsberg and G. Simpson, Phys. Rev. B 2, 1657 (1970).
[17]C. J. Palin, Proc. R. Soc. London Ser. A 329, 17 (1972).
[18]R. G. Poulsen, D. L. Randles, and M. Springford, J. Phys. F 4, 981 (1974).
[19]F. C. Hirschkoff, O. G. Synko, and J. C. Wheatley, Phys. Rev. Lett. 33A, 19 (1970).
[20]C. M. Hurd and J. E. Alderson, Phys. Rev. B 4, 1088 (1971).
[21]B. Knecht, G. G. Lonzarich, J. M. Perz, and D. Shoenberg, J. Low Temp. Phys. 29, 499 (1977).
[22]R. H. Hendel, Ph.D. thesis, University of Oregon, 1979 (unpublished). Available on microfilm through University Microfilms, Ann Arbor, Mich.
[23]B. G. Mulimani, Ph.D. thesis, McGill University, 1975 (unpublished).
[24]R. Harris, B. G. Mulimani, and M. J. Zuckermann, Phys. Condens. Matter 19, 269 (1975).
[25]H. Shiba, Prog. Theor. Phys. 50, 1797 (1973).
[26]H. Rohrer, J. Appl. Phys. 40, 1472 (1969).
[27]Y. Chung, D. H. Lowndes, C. Lin-Hendel, and J. P. Rohde, Solid State Commun. 20, 101 (1976).
[28]M. D. Daybell and W. A. Steyert, Phys. Rev. Lett. 20, 195 (1968).
[29]D. H. Lowndes and Y. Chung, Phys. Condens. Matter 19, 285 (1975).
[30]P. T. Coleridge, Phys. Rev. B 7, 3508 (1973).
[31]R. J. Higgins and R. H. Hendel, Solid State Commun. 39, 47 (1981).
[32]This field dependence is emphatically *not* a crystal substructure dephasing error. The neck orbit is quite insensitive to a substructure far larger than that present in our samples. Belly rotation diagrams which are a sensitive probe for crystal substructure showed no evidence of such a problem.